An Example of Interaction Between Finite-Amplitude Gravity Waves[1,2]

DAVID D. HOUGHTON[3]

University of Washington, Seattle, Wash.

(Manuscript received 15 June 1964)

ABSTRACT

An incompressible, stratified, hydrostatic, inviscid fluid model is used to demonstrate non-linear effects in the interaction of finite amplitude gravity waves. A statically stable density stratification is approximated by the superposition of ten homogeneous fluid layers with a very deep layer on top. Computations are made using a two-step Lax-Wendroff finite difference system. The solutions reveal intrawave distortions comparable to those predicted by analytical studies of one- and two-layer fluid models. During the interaction of two waves, the solutions show overall changes in wave speed which are of the same magnitude as the variations in wave speed that cause the intrawave distortions. These changes are related differently to the horizontal fluid velocities in the waves.

1. Introduction

In this study an attempt is made to demonstrate some effects of the non-linear properties of fluid motions. The non-linear advection terms in the equations of motion for fluid dynamics constitute a very conspicuous difficulty in the general analysis of fluid motions. The effect of advection must be considered in most atmospheric motion problems because the low viscosity of air allows large fluid velocities to exist. The analysis of such non-linearity requires that the fluid model considered be simple. For the analysis to be presented, the model consists of an adiabatic, incompressible fluid in a non-rotating coordinate system with no gradients in one horizontal coordinate direction. This model admits gravity waves which must be of finite amplitude in order to have non-linear effects.

Finite amplitude external gravity waves have been extensively analyzed for steady-shape solutions, both periodic and solitary, and non-steady-shape solutions. Lamb (1945) outlined the essential contributions of the earlier investigators which primarily concerned the steady-shape solutions. The steady-shape solutions indicate that some sort of relationship may exist between the advection terms and the non-hydrostatic pressure field such that there are no distortions occurring within the wave.

For this study, the horizontal scale of the motions is considered much greater than the vertical scale. This means that the gravity wave motions come under the classification of shallow fluid motions. Ursell (1953) has shown that if the hydrostatic assumption is made, such gravity waves will always propagate with a change of shape unless a quantity, $\eta_0\lambda^2/h^3$, is small, in which η_0 is the wave amplitude, λ is the wavelength, and h is the mean fluid depth. In the present analysis the wave amplitude is an order of magnitude smaller than the vertical scale in the fluid and the dominating wavelengths are more than one order of magnitude larger than the vertical scale. Thus the quantity, $\eta_0\lambda^2/h^3$, is much greater than 1. Therefore, the effect of the non-linear advection terms can be seen as distortions within the gravity waves in the fluid. This investigation is concerned primarily with such distortions and displacements in gravity waves.

Many studies have been made of such distortions in simple fluid models. Lamb (1945) briefly mentioned some earlier studies which were concerned with a one-dimensional compressible fluid. Courant and Friedrichs (1948) and Stoker (1957) gave a rather complete discussion of the distortions that occur in a homogeneous, incompressible, two-dimensional fluid due to the non-linear advection terms. Tepper (1952) and Freeman (1948) discussed atmospheric pressure jumps and easterly waves using essentially the same model. Tepper (1952) used a very deep homogeneous fluid layer above the fluid layer of interest to have wave velocities in the lower fluid with magnitudes comparable to the atmospheric situation. His discussion still concerned only a single layer fluid because the upper layer was considered so deep that fluid displacements at the top surface of the upper fluid were negligible and the horizontal pressure gradients in the lower fluid due to these were negligible.

[1] Contribution No. 88, Dept. of Atmospheric Sciences, University of Washington.

[2] The research reported in this paper is based partially on a Ph.D. dissertation, Department of Atmospheric Sciences, University of Washington, Seattle, Wash.

[3] Present affiliation: National Center for Atmospheric Research Boulder, Colo.

Wave distortions due to the non-linear advection effects have been studied in two-layer models, where the two homogeneous layers represent the first approximation to a stratified fluid and permit the representation of mean wind shear. In such models internal gravity waves can exist, and these have wave speeds less than those of the external waves. Long (1956) presented an analysis of distortions in waves in a two-layer model and showed how the distortions depended upon both the relative thickness of the two layers and the mean velocity shear. In the present study, the complicating effects of velocity shear are avoided by assuming no mean motions. Abbott and Torbe (1963) considered a model with stratification approximated by many homogeneous layers. They developed the general equations for such a model with an incompressible fluid and hydrostatic pressure; however, they analyzed the situation in more detail for the two-layer case only.

All of these studies have been concerned with the non-steady shape characteristics of a single wave. It is believed that the interaction between waves can add further insight to the nature and effect of the non-linear advection terms. An analysis of such effects is attempted here. Interaction between waves can be observed if the waves travel at different speeds and intersect each other. In a hydrostatic fluid this is possible only if the fluid is stratified, permitting the existence of many wave modes, internal waves, which will have differing wave speeds.

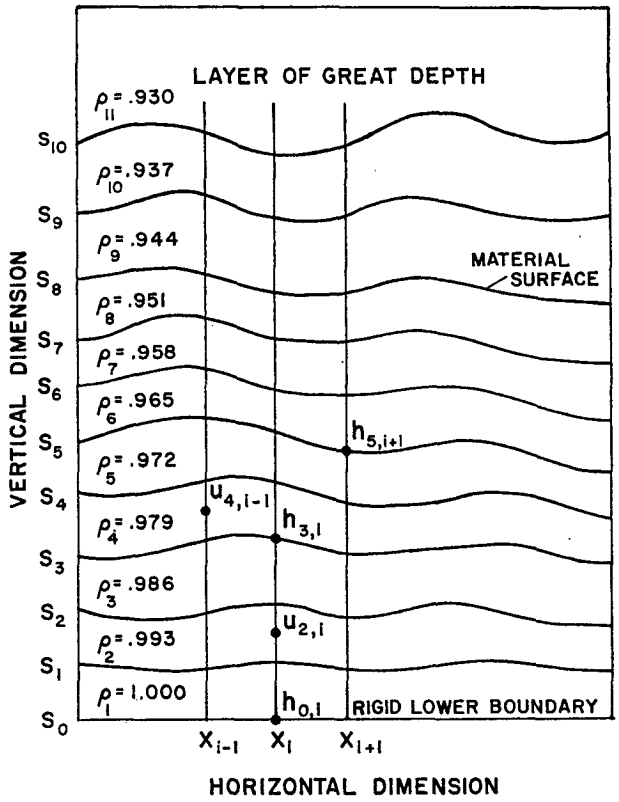

FIG. 1. Semi-Lagrangian model employed in the study. The location of some subscripted variables is shown. The material surfaces separating the layers are identified by S.

2. The physical model

The fluid considered is incompressible, non-viscous, and in hydrostatic balance at all times. Energy exchange is adiabatic, and the coordinate system is stationary and Cartesian. Homogeneity in the y-coordinate direction permits a complete representation of the motions in the vertical x-z plane. Stratification is approximated by eleven layers, each homogeneous in density with values such that a stable and linear stratification is represented. Fig. 1 illustrates this model.

The lower boundary is flat and rigid; the upper boundary is free. The top layer has a thickness so much greater than any other vertical scale in the model that displacements at the upper boundary may be ignored. Thus, only the density of the top layer is important to the wave motions which are completely described by the ten layers. This is done to permit relatively small percentage variations of density in the ten lower layers and yet to have a first mode wave speed in the ten layers that is less than an order of magnitude larger than some of the higher mode wave speeds. The small percentage variation in density simplifies the linear analysis of the model, and the closeness in wave speeds permits the first and second mode waves to interact for a reasonable length of time.

These simplifications make the model very restricted in its applicability to atmospheric motion systems, but such an unsophisticated model is necessary in order to single out effects of the non-linear advection terms. It is believed that effects of the non-linear processes demonstrated in such a simple model give more understanding of what their implications may be in reality.

3. Basic equations

The equations that describe the motions in this model are

$$\frac{\partial u}{\partial t}+u\frac{\partial u}{\partial x}+w\frac{\partial u}{\partial z}=-\frac{g}{\rho}\int_z^H\frac{\partial \rho}{\partial x}dz, \tag{1}$$

$$\frac{\partial u}{\partial x}+\frac{\partial w}{\partial z}=0, \tag{2}$$

$$\frac{\partial \rho}{\partial t}+u\frac{\partial \rho}{\partial x}+w\frac{\partial \rho}{\partial z}=0 \tag{3}$$

in which the symbols have the following meanings:

x: horizontal space coordinate
z: vertical space coordinate
t: time
u: velocity in x-direction

w: velocity in z-direction
ρ: density
g: acceleration of gravity
H: height of the upper boundary.

Since the model consists of layers of homogeneous fluid, it is instructive to convert the above set of equations to a semi-Lagrangian or material layer coordinate system such as discussed by Starr (1945) and Eliassen (1962). If the material surfaces are isopycnics, the conversion to the finite-layered model is direct. The semi-Lagrangian equations may be written:

$$\frac{\partial u}{\partial t}+u\frac{\partial u}{\partial x}=+\frac{g}{\rho}\int_z^H \frac{\partial \rho}{\partial z}\frac{\partial h}{\partial x}dz, \tag{4}$$

$$\frac{\partial}{\partial z}\left(\frac{\partial h}{\partial t}\right)+\frac{\partial u}{\partial x}+u\frac{\partial}{\partial z}\left(\frac{\partial h}{\partial x}\right)=0 \tag{5}$$

where h refers to the heights of material surfaces and derivatives of velocity are computed on the material surfaces.

In the model with eleven layers, the homogeneity of density in each layer and the absence of velocity shear within each layer means that the semi-Lagrangian equations can be integrated over the vertical dimension to give the following equations with x and t the only independent variables:

$$\frac{\partial u_k}{\partial t}+u_k\frac{\partial u_k}{\partial x}-\frac{g}{\rho_k}\sum_{\nu=k}^{10}\left[(\rho_{\nu+1}-\rho_\nu)\frac{\partial h_\nu'}{\partial x}\right]=0, \tag{6}$$

$$\frac{\partial h_k'}{\partial t}+\sum_{\nu=1}^{k}\left[u_\nu\frac{\partial(h_\nu'-h_{\nu-1}')}{\partial x}\right]+\sum_{\nu=1}^{k}\left[(h_\nu'-h_{\nu-1}')\frac{\partial u_\nu}{\partial x}\right]+\sum_{\nu=1}^{k}\left[(\bar{h}_\nu-\bar{h}_{\nu-1})\frac{\partial u_\nu}{\partial x}\right]=0. \tag{7}$$

In these the subscripts identify the layer, 1 being the lowest layer and 11 the very deep top layer. The symbol k ranges from 1 to 10 and ν is a dummy variable for k. Mean height, $\bar{h}$, and displacement h' at the top of the layer are subscripted the same as the velocity and density in the layer. The variables $\bar{h}_0$ and h_0' both refer to the rigid lower boundary and are zero. A set of equations equivalent to these was presented by Abbott and Torbe (1963). They made some general comments about the characteristics of the set of equations.

The non-linear terms of the original equations, $u(\partial u/\partial x)$ and $w(\partial u/\partial z)$ in (1), are now represented by $u_k(\partial u_k/\partial x)$ in (6) and

$$\sum_{\nu=1}^{k}\left[u_\nu\frac{\partial(h_\nu'-h_{\nu-1}')}{\partial x}\right]$$

and

$$\sum_{\nu=1}^{k}\left[(h_\nu'-h_{\nu-1}')\frac{\partial u_\nu}{\partial x}\right]$$

in (7). The height displacement, h', is related to the vertical motion, w by the kinematic relationship,

$$w_k=\frac{\partial h_k'}{\partial t}+u_k\frac{\partial h_k'}{\partial x} \tag{8}$$

where w_k is the vertical motion at the top of layer k.

4. General considerations

This study concerns motions which are only slightly non-linear. Therefore, at all times, the non-linear terms, while much smaller than the linear terms, are not negligible. Thus, some characteristics of the gravity wave motions may be described aptly by the linear equations. The distortions and differential wave displacements are small added effects.

A scale analysis of the set of equations (6) and (7) suggests the conditions for which the non-linear effects are small non-dimensional quantities are defined as $x^*=x/L$, $u^*=u/U$, $h'^*=h'/H'$, $\bar{h}^*=\bar{h}/\bar{H}$, $\rho^*=\rho/R$, $g^*=g/G$, and $t^*=L/c$. The capital letters are the scaling quantities, and c refers to the wave speed of the gravity waves. If these are substituted into (6) and (7) and if each equation is divided by the coefficient of its time derivative, it is observed that the non-linear terms are all multiplied by the scaling factor U/c which is the Froude number. This suggests that the relative importance of the non-linear terms can be indicated solely by the magnitude of a Froude number giving a ratio of fluid velocity magnitudes to wave speeds. Small non-linear effects are noted for values of the Froude number much less than 1.

5. Linear analysis

A linear analysis of this model indicates certain features of the waves that apply to the finite amplitude cases. For this analysis the lower ten layers are considered a continuous medium with a density profile given by $\rho=\rho_0-[(D/2)-z]\sigma$; the deep upper layer is homogeneous. Here $\sigma=\partial\rho/\partial z$ and is constant, and D is the total depth of the ten lower layers. For a statically stable condition σ must be negative. Since no mean velocity is considered, the displacement of the material surfaces, h', is related to the vertical velocity by $\partial h'/\partial t=w$.

The equations can be expressed in terms of three dependent variables, u, h', and p, where p is pressure and all three are perturbation quantities. The equations are

$$\frac{\partial u}{\partial t}=-\frac{1}{\rho_0-\left(\frac{D}{2}-z\right)\sigma}\frac{\partial p}{\partial x}, \tag{9}$$

$$\frac{\partial u}{\partial x}+\frac{\partial^2 h'}{\partial z \partial t}=0, \tag{10}$$

$$\frac{\partial p}{\partial z}=gh'\sigma. \tag{11}$$

Here, as in an analysis of a similar set of equations by Bolin (1953), density variations are subsequently ignored in the equation of motion and equations (9), (10), and (11) are combined to give a simple fourth order equation for h'. By assuming a solution which is periodic in the x-direction, the fourth-order equation and boundary conditions may be satisfied by waves with speeds satisfying the following transcendental frequency equation,

$$\tan\left[D\left(\frac{-g\sigma}{\rho_0 c^2}\right)^{\frac{1}{2}}\right]=\frac{-c^2\rho_0}{\Delta\rho g}\left(\frac{-g\sigma}{\rho_0 c^2}\right)^{\frac{1}{2}}, \tag{12}$$

where c is the wave speed, D is the depth of the stratified fluid, and $\Delta\rho$ is the density difference across the interface between the lower stratified fluid and the deep upper fluid layer.

This result is equivalent to that of Bolin (1953), and it shows that there are infinitely many wave solutions, each corresponding to a wave mode, the first mode having the largest wave speed. Because the model studied has only ten discrete layers to represent the stratified fluid, only the first ten wave modes can be represented. The frequency equation also shows that the wave speeds depend on the stability of the stratified region, density difference across the interface between the two regions of the fluid, the acceleration of gravity, and the total depth of the stratified fluid, but not on wavelength. It is expected that the wave speeds predicted by this analysis will be close to those in the small but finite amplitude waves. This linear analysis shows that gravity waves of different speeds exist in the model permitting study of interwave as well as intrawave non-linear effects.

6. Theoretical discussion

Most theoretical studies of non-linear effects in shallow fluid gravity waves have been made by employing the method of characteristics to solve the non-linear partial differential equations. This method of solution is discussed extensively by Courant and Friedrichs (1948). Stoker (1957) discussed the theoretical behavior of a single layer model. Tepper (1952) applied the solution of a one-layer fluid to a two-layer model by considering the upper layer so deep in comparison to the lower one that the system could be considered a one-layer fluid with a reduced value of gravity, the amount of reduction depending upon the ratio of the density between the two layers. Long (1956) and Abbott and Torbe (1963) studied two-layer models, again by the method of characteristics, where such an approximation was not made.

These studies have shown how each part of a wave may be considered to have a rate of propagation which depends on the intensity or a displacement of the wave at that particular part. Thus the non-linear terms are considered to have an effect on the wave speed. In the model under consideration, only the lower boundary is rigid, and the analysis by Long (1956) is less applicable than those by Abbott and Torbe (1963) and Tepper (1952). Tepper showed that for a two-layer model, the upper layer being infinitely deep, simple waves in the lower layer had a propagation speed of $u+[(1-\beta)gh]^{\frac{1}{2}}$ where u is the velocity in the lower fluid and h its depth at the point in question, while β is the ratio of densities in the two layers.

The analytic solutions have indicated a non-linear effect which is dependent both upon the horizontal and vertical fluid velocities, the latter being described in the discussion of vertical displacements. Tepper (1952) showed that for a single layer fluid, or one with a very deep layer above, the rate of propagation of a given position on a simple wave differed from that in a wave of an infinitely small intensity by an amount which was one and a half times the actual fluid velocity at that position. In other words, the change in wave speed due to its being of finite amplitude is a result of both the finite u-velocity and finite vertical displacement, the former accounting for two-thirds of the change and the latter for one-third.

7. Method of computation

Equations (6) and (7) were represented by finite differences and integrated numerically. The two-step Lax-Wendorff scheme described by Richtmyer (1963) was used. It is of second order accuracy and is easily formulated for the equations of this study.

Equations (6) and (7) can be represented in conservation-law form as shown:

$$\frac{\partial u_k}{\partial t}+\frac{\partial F_k}{\partial x}=0, \tag{13}$$

$$\frac{\partial(h_k-h_{k-1})}{\partial t}+\frac{\partial G_k}{\partial x}=0 \tag{14}$$

where

$$F_k=\tfrac{1}{2}u_k^2-\sum_{\nu=k}^{10}\left[g\left(\frac{\rho_{\nu+1}-\rho_\nu}{\rho_k}\right)\frac{\partial h_\nu}{\partial x}\right]$$

and

$$G_k=u_k(h_k-h_{k-1}).$$

These can then be written in the following finite difference form for the two-step Lax-Wendroff scheme used in the calculations:

$$u_{k,i,l+1}=\tfrac{1}{2}(u_{k,i+1,l}+u_{k,i-1,l}) -\frac{\Delta t}{2\Delta x}(F_{k,i+1,l}-F_{k,i-1,l}), \quad (15)$$

$$h_{k,i,l+1}=h_{k-1,i,l+1} +\tfrac{1}{2}[(h_{k,i+1,l}-h_{k-1,i+1,l})+(h_{k,i-1,l}-h_{k-1,i-1,l})] -\frac{\Delta t}{2\Delta x}(G_{k,i+1,l}-G_{k,i-1,l}), \quad (16)$$

$$u_{k,i,l+2}=u_{k,i,l}-\frac{\Delta t}{\Delta x}(F_{k,i+1,l+1}-F_{k,i-1,l+1}), \quad (17)$$

$$h_{k,i,l+2}=h_{k-1,i,l+2}+(h_{k,i,l}-h_{k-1,i,l}) -\frac{\Delta t}{\Delta x}(G_{k,i+1,l+1}-G_{k,i-1,l+1}). \quad (18)$$

The subscripts, k, i, and l refer to the layer, x-coordinate, and time, respectively, such that if θ is any variable, $\theta_{k,i,l}$ means $\theta_{k,i\Delta x,l\Delta t}$ or the θ associated with the kth layer at the x-coordinate $i\Delta x$ and at the time $l\Delta t$. The space and time increments are, respectively, Δx and Δt. Richtmyer (1963) showed that this scheme is stable for $[(c+|u|)\Delta t/\Delta x]<1$, the von Neumann stability condition. Here c is a wave velocity of the system and u a fluid velocity. The scheme dampens the short wavelengths which prevents the occurrence of non-linear instability.

The lower boundary was made rigid by prescribing the bottom surface of layer 1 to be at a height of 0 at all times. The upper boundary (actually the interface between the stratified region and the deep homogeneous layer above) was free which meant that its height was determined solely by the total convergence in the fluid layers beneath it. The left boundary was made rigid by setting the fluid velocity at zero and prescribing the slopes of all the material surfaces to be zero at the left boundary. Velocity and height displacement at the right boundary were computed by assuming that $\partial^3 u/\partial x^3$ and $\partial^3 h/\partial x^3$ were both zero at one and a half grid spacings in from the right boundary. The effect of these arbitrary lateral boundary conditions was minimized by making sure that the finite amplitude parts of the gravity waves remained well to the interior of the lateral boundaries for the entire period of the computations.

Because infinite horizontal gradients were an eventuality in this model, initial conditions had to be so prescribed that horizontal gradients would never approach infinity during the computations. This was achieved by using well behaved functions for the initial fields of velocity and height displacement and by prescribing initial gradients sufficiently small compared to the intensity of the wave systems.

The initial conditions for horizontal velocity and height of the material layers were given, respectively, by $u_{k,i}=A(k)\,\mathrm{sech}^2[(x_0-i\Delta x)/L]$ and $h_{k,i}=\tilde{h}_k+B(k)\times\mathrm{sech}^2[(x_0-i\Delta x)/L]$ where $A(k)$ and $B(k)$ are the amplitude factors, x_0 is the horizontal coordinate of the wave maximum, and L determines the width. The amplitude factors, $A(k)$ and $B(k)$, were determined by trial and error so that the resulting distributions would constitute primarily either a first or second mode wave traveling in one direction.

The waves so prescribed had half widths of about 18 grid spacings where the grid spacing was 8 km, and 200 grids represented the entire horizontal dimension of 1600 km. Each layer had a mean thickness of 300 m, and the density gradient was about -0.7 per cent per layer. This density gradient gives a stability approximating that of the U. S. Standard Atmosphere. Fig. 1 shows the density distribution in normalized units. Integrations were carried out for 216 time steps with a time increment of 200 seconds. Thus 12 hours of time were represented in the prototype.

8. Results of the computations

Three computations were carried out. In the initial computation a first mode wave was originated near the left side of the model which moved to the right. In the next, a second mode was originated to the left of center of the model which also moved to the right. In the third, both waves were originated each as just described. The top diagram in Fig. 2 shows the initial conditions for the third computation. The first mode wave is nearest the left boundary. The initial conditions for the first and second computations are the same as those represented in the top diagram but with the wave on the right or left, respectively, missing.

Integrations were carried out for 12 prototype hours in each computation. In the first computation, the first mode wave moved to the right boundary during this time; while in the second, the second mode wave moved from left of center to the right of center of the model. In the third, where both waves were present, each wave traveled about the same distance as in its preceding computation and intersected during the computation. Fig. 2 shows the results of the third computation. The top diagram is the initial condition; the middle diagram shows the two wave modes in superposition at 5 hours; and the lower diagram shows the waves again clearly separate at 10 hours, but now with the first mode wave on the right side.

In the computations, the waves move approximately at the speed predicted by the preceding linear analysis. Distortions within each wave are similar to those theoretically determined for single layer models. The increase in rate of wave displacement, over that of a wave with infinitely small intensity, is proportional to and of the same order of magnitude as the vertically averaged u-velocity existing at that point. Since the vertically

averaged u-velocity in each wave is in the same direction as the wave motion, the most intense center portion of each wave moves faster than the extremities and initially symmetric waves become asymmetrical with gradients increasing on the leading edge of the wave. Gradients in the first mode wave approximately double over the course of the computations, but even at the end their magnitude still indicates vertical accelerations that are less than 0.1 per cent of the acceleration of gravity. Thus at no time is the hydrostatic assumption inappropriate. Fig. 3 shows the time-space position of certain parts of the first and second mode waves in the three computations. For each wave the center line is the most intense portion and the two outer lines are the points where the wave is one tenth as intense. The latter move approximately as described by linear analysis.

The distortion within the waves is analogous to that theoretically determined for a wave in a homogeneous fluid. The analogy even extends to the amount by which the rate of propagation is increased. In each wave mode the vertical average of u-velocity, $\int_0^D u dz$, where D is the total depth of the ten layers, is about equal to the increase in propagation rate over that of waves of infinitely small intensity. The velocity does not change direction with height in the first mode wave as it does in the second; thus even though magnitudes are comparable in both cases, the first mode wave has a much larger differential in wave popagation rates between its most and least intense portions than does the second mode wave. Tepper (1952) indicated that the increase in propagation rates should be one and a half times the fluid velocity instead of being equal to it.

The effect of interaction between the two waves is observed by comparing the positions of the two waves in the third computation with those in the first two computations where no interaction occurred. Fig. 3 shows the position of each wave in both cases. During the interaction, wave speeds were altered so that, after intersecting, the first mode wave lagged behind its position in the no-interaction case and the second mode wave was ahead of its position in the no-interaction case. The dashed lines in Fig. 3 show the resulting displaced positions. The total net displacement due to this interaction was constant throughout each wave as shown in Fig. 4. This figure uses the vertical displacement at the top of the stratified layer as an indicator of the wave position after 10 hours.

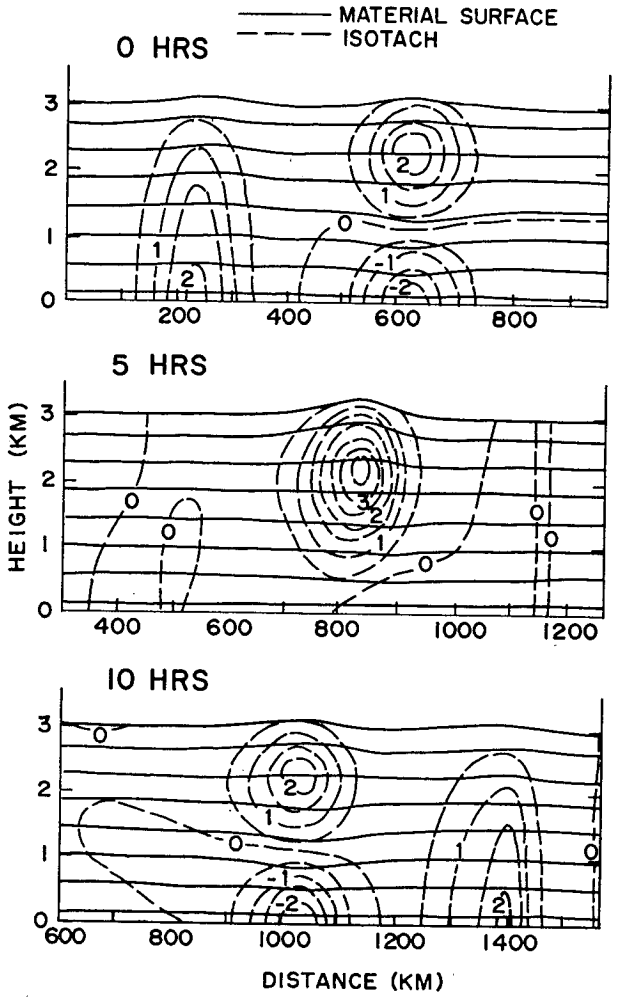

FIG. 2. The numerical solution for the third computation showing the interaction of the first and second mode waves. The top diagram shows the initial conditions, the center diagram the waves after 5 hours, and the lower diagram the waves after 10 hours. Isotachs are labeled in units of m sec^{-1}. The abscissa is the distance from the left boundary.

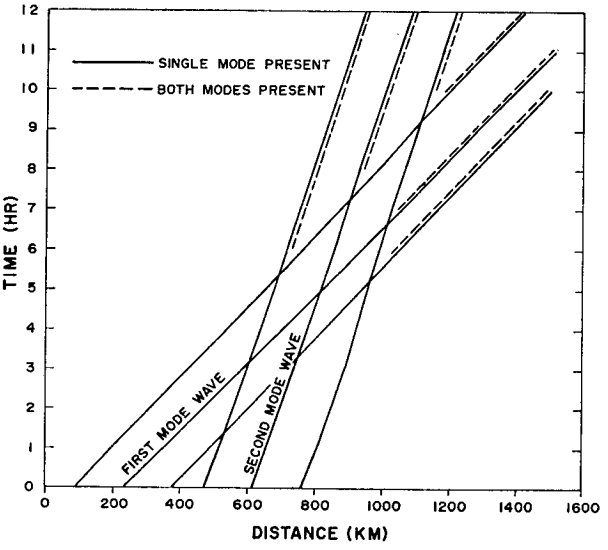

FIG. 3. Wave positions in x-t space of the first and second mode waves. The solid lines apply to the first and second computations, the dashed lines to the third computation. The center line in each wave locates the most intense portion of the wave, and the other lines locate points where the intensity is one tenth as great in each wave, respectively.

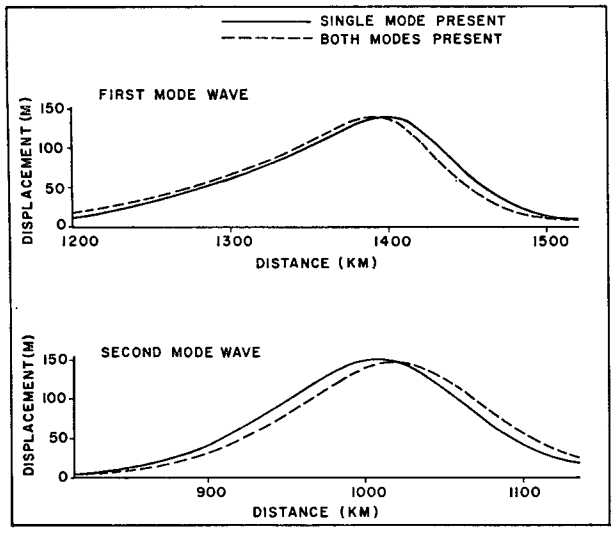

FIG. 4. Vertical displacement at the top of the stratified layers 10 prototype hours after the computations commenced. Both the first and second mode waves are illustrated for the no-wave-interaction and the wave-interaction cases.

The displacement due to this interaction seems to be insignificant in Fig. 3, but if the interaction time is considered to be about 4 hours, the displacements indicate changes in wave speed during this time of interaction which are of about the same magnitude as those at the most intense portion of each wave caused by its finite amplitude condition. In each case, wave speeds are altered by amounts ranging up to 10 per cent of the magnitude of the linear wave speed.

The central fact to be noted is that although the most intense region in each wave is moving forward relative to its less intense portions, the interaction between the waves causes one wave to move forward while the other moves back relative to the movement that occurs when no interaction takes place between the waves. This non-linear effect and those occurring in single waves illustrate the differing effect of the horizontal and vertical advection terms. These differences are suggestive of the complexities of the non-linear advection terms in real fluid motions. The fact that changes in wave velocities in the interwave interactions are in opposite directions demonstrates a conservation of momentum for the system consisting of the two waves.

Two independent checks on the computations were provided by the linear analysis and the energy condition in the model. In computations, both the first and second mode waves had wave speeds in their less intense portions which were about 5 per cent less than the respective wave speeds determined by a linear analysis of the model. In each computation, the total energy content of the model remained nearly constant. The total kinetic energy of the system varied no more than 3 per cent in each of the computations. Without energy sinks or sources in the model, the total energy would be expected to remain constant, and with essentially only simple waves present, the total kinetic energy would be expected to remain constant.

Acknowledgments. Appreciation is expressed to Dr. Robert G. Fleagle, University of Washington, for his guidance in the dissertation on which this paper is based and to Dr. George Platzman, University of Chicago, and Dr. Akira Kasahara, National Center for Atmospheric Research, for their useful comments and discussions. The Weather Bureau General Circulation Research Laboratory kindly assisted with some of the calculations. The final calculations were performed at the National Center for Atmospheric Research. A part of the research was financed by NSF grant G3991. Help on the manuscript was given by my faithful wife, Barbara.

REFERENCES

Abbott, M. B., and I. Torbe, 1963: On flows and fronts in a stratified fluid. *Proc. Roy. Soc., Series A*, **273**, 12–40.

Bolin, B., 1953: The adjustment of a non-balanced velocity field towards geostrophic equilibrium in a stratified fluid. *Tellus*, **5**, 373–385.

Courant, R., and K. Friedrichs, 1948: *Supersonic flow and shock waves*. New York, Interscience Publishers, 464 pp.

Eliassen, A., 1962: On the use of a material layer model of the atmosphere in numerical prediction. *Proc. of the Internat. Symposium on Numerical Weather Prediction*, Tokyo, Meteor. Soc. of Japan, pp. 207–211.

Freeman, J. C., 1948: An analogy between the equatorial easterlies and supersonic gas flows. *J. Meteor.*, **5**, 138–146.

Lamb, H., 1945: *Hydrodynamics*. New York, Dover Publications, 738 pp.

Long, R. R., 1956: Long waves in a two-fluid system. *J. Meteor.*, **11**, 70–74.

Richtmyer, R. D., 1963: *A survey of difference methods for non-steady fluid dynamics*. NCAR Tech. Note 63-2, National Center for Atmospheric Research, Boulder, Colo., 25 pp.

Starr, V. P., 1945: A quasi-Lagrangian system of hydrodynamical equations. *J. Meteor.*, **2**, 227–237.

Stoker, J. J., 1957: *Water waves*. New York, Interscience Publishers, 567 pp.

Tepper, M., 1952: *The application of the hydraulic analogy to certain atmospheric flow problems*. Washington, D. C., U. S. Weather Bureau, Research Paper No. 35, 50 pp.

Ursell, F., 1953: The long-wave paradox in the theory of gravity waves. *Proc. Cambridge Phil. Soc.*, **49**, 685–694.